Photoreflectance of a 2.3μm GaInAsSb-based VCSEL structure for gas sensing applications

G. M. T. Chai[1], T. J. C. Hosea[1, 2], N. E. Fox[2], K. Hild[2], A. B. Ikyo[2] I. P. Marko[2], A. Bachmann[3], S. Arafin[3], M.-C. Amann[3] and S. J. Sweeney[2]

[1]*Ibnu Sina Institute for Fundamental Science Studies, Universiti Teknologi Malaysia, Johor Bahru* 81310, *Malaysia*
[2]*Advanced Technology Institute and Department of Physics, University of Surrey, Guildford, GU2 7XH, UK*
[3]*Walter Schottky Institut, Technische Universität Munchen, Am Coulombwall 4, D-85748 Garching, Germany*

***Abstract*— Temperature-dependent photo-modulated reflectance (PR) spectroscopy has been applied to study a GaSb-based vertical-cavity surface-emitting laser (VCSEL) structure designed to operate at 2.3μm. To investigate the wavelength offset between the quantum well (QW) and cavity mode (CM) features, which determine the device's physical properties and temperature performance, the energies of the QW transitions relative to the VCSEL CM energy were tuned by heating from 9K to 300K. We found that this VCSEL structure has a QW-CM offset of 21meV at room temperature; also, the QW ground-state transition only comes into resonance with the CM at 220±2K. These PR results are closely compared with those obtained in a separate study of actual operating devices.**

Keywords*— *VCSEL, mid-infrared, photo-modulated reflectance, spectroscopy, gas sensing.

I. INTRODUCTION

Mid-infrared (mid-IR) gas sensing uses tunable diode laser absorption spectroscopy, with distributed feedback (DFB) lasers being currently preferred due to their single transverse and longitudinal mode operation with narrow linewidths. However, these lasers are comparatively expensive, have high power consumption, and have a highly asymmetric beam-profile which requires additional beam control optics, adding cost and complexity to the package[1, 2]. In contrast, mid-IR GaSb-based vertical-cavity surface-emitting lasers (VCSELs) have symmetrical beam profiles which make the optical system much simpler and cheaper. At the same time, VCSELs have single longitudinal mode operation, low threshold currents, and low power consumption due to a high thermal resistance, and so could be improved replacements for DFB lasers[1-4]. The major challenge in achieving efficient lasing in VCSELs is strongly dependent on the wavelength alignment between the peak of the gain spectrum of the active quantum well (QW) layers and the cavity mode (CM) of the reflectance spectrum of the VCSEL Fabry-Perot structure. When other effects such as self-heating and non-radiative recombination is taken into account, achieving an optimized alignment at the desired operating temperature (T) between the energy positions of the QW ground-state transition (E_{QW}) and the CM dip in the reflectance spectrum (E_{CM}) should give ideal device performance[5, 6]. However, even a small E_{QW}-E_{CM} misalignment at the desired operating T causes significant degradation in the threshold current and output power. So, it is important to monitor the degree of any such misalignment, preferably before one has gone to the trouble of fabricating the devices from the as-grown VCSEL structure wafers, for example, so that the optimum wafer positions can be determined. Here we report on the optical spectroscopic characterisation of pre-fabrication 2.3μm GaSb-based VCSEL structures. We do this with the aim to determine the E_{QW}-E_{CM} detuning of this structure without having to process them into working devices. We use the well known powerful non-destructive, non-contact photo-modulated reflectance (PR) method of studying the E_{CM}/E_{QW} alignment in VCSEL structures, as functions of incidence angle and T. This technique also allows us to directly monitor the QW transition energies of the full VCSEL structure[7]. As a comparison, a corollary sample with the top distributed Bragg reflector (DBR) removed by etching is used, which was already prepared for photoluminescence studies. We also compared our conclusions closely with the results of a separate study of the performance operating devices made from the same wafer structures[3].

II. SAMPLE AND EXPERIMENTAL DETAILS

The type I VCSEL GaInAsSb/AlGaAsSb/GaSb wafers, aimed to emit at ~2.33μm at room temperature (RT), were grown by molecular beam epitaxy to the following structure: n-doped GaSb substrate; 24-pair n-doped bottom $AlAs_{0.09}Sb_{0.91}$/GaSb DBR; five 11nm 1.6% compressively-strained $Ga_{0.63}In_{0.37}As_{0.11}Sb_{0.97}$ QWs, sandwiched between 8nm $Al_{0.33}Ga_{0.67}As_{0.03}Sb_{0.97}$ barriers; strongly doped p+ GaSb/n+ InAsSb buried tunnel junction (BTJ) (for optical/current confinement) ; and top DBR of a Si/SiO_2[2, 3]. The intention of the BTJ is to improve the current injection so reducing the resistive heating and absorption loss within the VCSEL (n-doped material has lower free carrier absorption) and giving a higher electrical conductivity. Despite this, the VCSELs had relatively poor performance (2.6kA/cm^2 threshold current density, 2% differential efficiency, 87μW maximum power output[1]). Minimum threshold current and maximum output power were at -10^{0}C. Reference [2] comments that this may be due to E_{QW}-E_{CM} detuning. We check this here using PR, studying two samples: sample A is a 2.5cm strip of full VCSEL structure wafer; sample B is the aforementioned sample with the top DBR removed. Due to growth conditions the E_{CM} in sample A varied across the 2.5cm radius of the wafer, blue-shifting by 25nm from the wafer centre to its edge.

PR is a non-destructive, contactless and yet most sensitive spectroscopic technique that externally modulates the complex dielectric function, $\varepsilon_1+i\varepsilon_2$, of the sample using a chopped laser pump source which in turn modulates the sample reflectivity R. We used the setup described in [7] which allowed us to measure R and ΔR simultaneously in the VCSEL structures. PR can give not only a direct determination of E_{CM} from the R spectrum, but may also allow the E_{QW} to be measured, or inferred by varying some external parameter, thus revealing the extent of the alignment of E_{CM} and E_{QW} – an attribute very important to successful device operation[7]. Initially we measured RT R spectra on sample A as a function of incidence angle, θ, from 21^0 to 85^0 using a single-grating spectrometer, tungsten filament lamp, lock-in amplifier and cooled InSb detector. A mechanical chopper set at 333Hz was placed in front of the spectrometer exit slit so that the light that was to be reflected off the sample was then possible to be detected using lock-in amplification with less background noise. These measured R were then normalised by dividing them by the set-up system response. For the T variation PR, the T was varied from 9K to 300K at a fixed $\theta = 45^0$. Both samples were modulated with a 808nm, 450mW GaAlAs diode laser electrically chopped at 812Hz. The samples were mounted in a closed cycle helium cryostat; cooled down to 9K and were heated in suitable steps to measure a sequence of PR spectra up to RT using the same spectrometer, detector and lock-in arrangement described above for the angle-dependent R measurements.

III. Theoretical Background

In PR, the AC component of R, ΔR, has sharp derivative-like forms revealing the sample's electronic transition energies; uninteresting broad backgrounds in R are removed[7, 8]. When the laser is on, carriers are excited, drift in the built-in electric field and get trapped in various centers, which in turn decreases the field. When the laser is off, the carriers are released from the traps, and the field is restored to its original value. This mechanism of modulating internal electric fields gives periodic changes in the sample's complex dielectric function, $\boldsymbol{\delta}\varepsilon_1+i\boldsymbol{\delta}\varepsilon_2$ and, thus, yield the relative changes in reflectivity, ΔR/R, which is defined the PR signal by [7]:

$$\Delta R/R = \alpha\delta\varepsilon_1 + \beta\delta\varepsilon_2 \qquad (1)$$

Equation (1) describes the relative changes in the sample R due to the applied oscillating electric field (via the chopped laser) where $\delta\varepsilon_1$ and $\delta\varepsilon_2$ are the modulated QW dielectric function line-shapes and can be expressed for instance by the Aspnes third derivative functional form (TDFF)[9]. α and β are the Seraphin coefficients which in simple heterostructures with relatively few layers are nearly energy independent compared to $\delta\varepsilon_1$ and $\delta\varepsilon_2$. However, VCSEL PR spectra α and β strongly vary, especially when in the vicinity of the VCSEL CM dip, and a modified form of (1) is required to model the PR, as described in detail in [10], which accounts for the energy dependence of α and β. Both pairs of parameters in (1) - $\delta\varepsilon_1$ and $\delta\varepsilon_2$, and α and β - form Kramers-Kronig pairs so that, while α has an anti-symmetric shape near E_{CM}, β has a symmetric form. In contrast, $\delta\varepsilon_1$ has an essentially symmetric form near E_{QW} while $\delta\varepsilon_2$ is anti-symmetric[6, 7]. The product of these pairs of lineshapes in (1) results in a rather complicated interplay between the symmetries and intensities of the four features. However, this can be written down in a suitable analytical form that can be used to fit the measured VCSEL PR spectra[9].

IV. Results and Discussions

A. Angle dependent reflectivity

When $E_{QW} > E_{CM}$ at RT, it may be possible to tune E_{CM} to move into resonance with E_{QW} by changing the angle of incidence θ of the spectrometer light being shone onto the front surface of the VCSEL structure. Increasing θ causes the CM dip to blue-shift according to:

$$\lambda_{CM}(\theta) = \lambda_{CM}(0^0)\sqrt{1-\frac{\sin^2(\theta)}{n_{eff}^2}} \qquad (2)$$

with $\lambda_{CM}(0^0)$ the normal incidence CM wavelength, and n_{eff} the refractive index of the effective cavity[8]. Meanwhile, the E_{QW} is independent of θ. The CM dip energy measured here showed the expected blue shift with increasing angle as predicted. As suggested by (2), the square of the λ_{CM} (θ) results obtained were plotted against the square of sine of θ and the results fitted to give a very satisfactory straight line fit with $\lambda_{CM}(0^0)$ = 2.329±0.001μm, and n_{eff} = 3.433±0.003. This fit was later used to obtain λ_{CM} at other θ using linear extrapolation. As we increased θ, and the E_{CM} blue shifted, we also observed that the normalised reflectivity spectra started to show changes in the CM dip profile, in both the depth and shape of the CM dip. The CM was observed to have the deepest, most symmetric dip, at ~0.544eV (~2.28 μm) at an incidence angle of 45±5° (at RT). Such a condition is sometimes interpreted as being an indication that E_{CM} and E_{QW} are in alignment at this angle[9]. However, as discussed later, this initial finding is insufficient to draw this conclusion[6].

B. Temperature dependent reflectivity and photo-modulated reflectance

Studying the PR spectra as a function of temperature can give more detailed information about the relative positions of E_{CM} and E_{QW} as both energies increase with cooling. E_{QW} increases due to the variation of the fundamental band gap energy with temperature. Decreasing the temperature decreases the refractive index of the materials within the active region, as well as causing physical shrinkage, thus decreasing the cavity optical thickness (which together determines the CM wavelength). Thus E_{CM} also increases with cooling, but generally rather more slowly than E_{QW}[9].

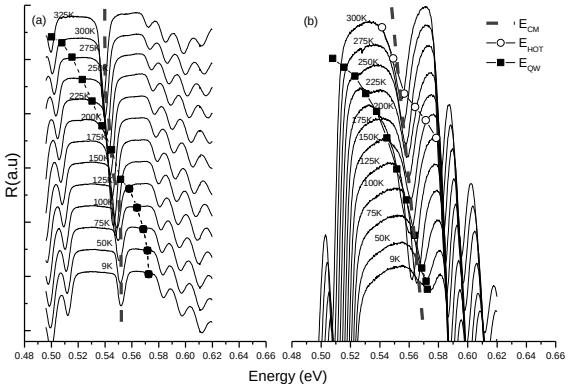

Figure. 1 Variable T normalized R spectra for samples (a) A and (b) B, at 45^o incidence angle. Dashed line shows CM dip position E_{CM} . Black squares and open circles show E_{QW} and E_{HOT} from PR fits, respectively. E_{CM} and E_{QW} blue shift with cooling, E_{CM} more slowly than E_{QW}, becoming tuned at ~175K and ~100K for samples A and B, respectively.

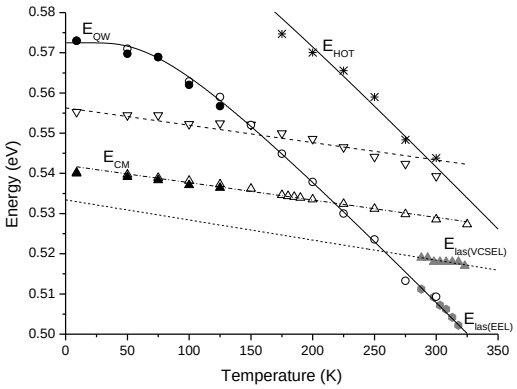

Fig. 3 T-dependence of E_{CM} (triangles), E_{QW} (circles) and E_{HOT} (stars) for samples A (filled symbols) and B (open symbols). Curves are BE fits to E_{QW} & E_{HOT}. Straight lines are fits to E_{CM} with slope 0.043±0.002meV/K for both samples A and B. Grey symbols are VCSEL and EEL results of [3].

Figs. 1(a) and 1(b) show the normalized R spectra from 9K to 325K, for samples A and B, respectively. For the etched sample B, the CM dip results only from the bottom DBR, and is higher (~0.57eV at 9K) than in sample A (~0.55eV). E_{CM} increases with cooling due to changes in n_{eff}, and physical shrinkage at a rate of 0.043±0.002meV/K for both A and B (see later). For information, Fig. 1 also shows the positions of the QW transition energies determined from PR fits (discussed later). E_{QW} increases with cooling via the band gap energy (but faster than E_{CM} at ~29.2meV/K)). Since E_{QW}<E_{CM} at RT, then E_{QW} crosses and comes into resonance with E_{CM} with increase of T[6, 7, 9]. In the PR of sample B we were also able to observe a QW higher-order transition (HOT), E_{HOT}, at ~0.58eV (at 175K) and the PR fitted energies for this are also shown in Fig. 1(b), by the open circles. Figs. 2(a) and (b) show the associated PR spectra. The solid curves are fits with the model in [10] for (1). Both samples' PR show a strong oscillation associated with the CM dip (dashed line, E_{CM} = ~0.55eV at 9K in sample A). Sample A has a higher energy feature (filled squares) which we interpret as E_{QW}, but which became unobservable above 125K. In sample B the CM feature is less obvious, but there are two strong features (filled squares and open circles) due to two QW transitions observable up to 300K. In both samples E_{QW}≈0.57eV at 9K. In sample B, E_{QW} decreases with increasing T and crosses E_{CM} at ~100K at ~0.565eV. At 175K, the E_{HOT} appears at ~0.57eV in sample B (open circles) which also moves and crosses E_{CM} at ~250K at ~0.56eV.

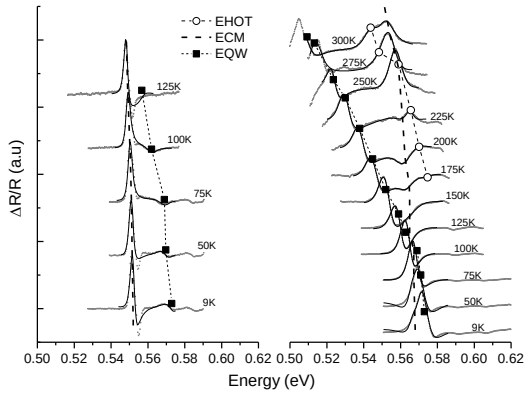

Fig. 2 The T-dependent PR spectra of samples (a) and (b). Filled squares show E_{QW}. Open circles show E_{QW}. Dashed lines show E_{CM}. Full curves are fits with VCSEL PR model of [10].

Fig. 3 summarises the T-dependent results of the measured and fitted energies. E_{CM} and E_{QW} for samples A and B agree well. All the PR spectra were measured at a 45^o incidence angle but in Fig. 3 all the E_{CM} results have been shifted to normal incidence values using the aforementioned linear fit of (2) to the angle dependent normalised RT R spectra results. The lines passing through the E_{CM} results for both samples are linear fits giving slopes, as mentioned earlier, of 0.043±0.002meV/K in both samples. The circles in Fig. 3 represent the E_{QW} results: the filled circles are those obtained from fitting the PR spectra of sample A, and the open circles are the corresponding fitted PR results from sample B. These are clearly in good agreement. The curve passing through the E_{QW} results is a fit with a Bose-Einstein (BE) model [11]:

$$E = E_o - 2\alpha_B / [\exp(\theta_B/T)-1] \qquad (3)$$

with E_0 = 0.5725±0.0008eV; θ_B = 223±19K and α_B = 35±4meV. We may also note that the E_{CM} results for sample B are ~15meV higher than in sample A. A further study by measuring the RT reflectivity spectra as a function of wafer position across the sample A wafer strip showed that this is caused by two factors: unintended growth variations across both wafers, especially when sample B was taken from the wafer edge; and removal of the sample B top DBR may have altered the observed E_{CM} position. The stars in Fig. 3 show the fitted E_{HOT} PR results for sample B and the curve is the same E_{QW} BE fit, but shifted up by 35meV. The fits to the sample A E_{CM} and E_{QW} results cross at T=220±2K at energy ~0.532eV. Thus, the prediction from the PR is that the VCSEL will indeed lase at

~2.3μm, but the ideal operating T is 220K, well below the desired RT value. In fact, an ideal VCSEL requires $E_{QW}>E_{CM}$ at RT, so that they align when the device heats up due to the driving current.

C. Comparison of photo-modulated reflectance results with device studies.

Fig. 3 also compares results from [3] of the emission energy, $E_{las(EEL)}$, of an edge-emitting laser (EEL) with similar active region to the VCSEL (grey circles).* The $E_{las(EEL)}$ increases with cooling at a rate of 0.30meV/K, as shown by the solid line to the lower right in Fig. 3. [3] also concluded that E_{QW} and E_{CM} come into resonance in the operating VCSEL device at ~263K and at 2.38μm and that, at RT, the CM is actually detuned by ~+10meV from the QW gain peak in the VCSEL device. Being unaffected by any DBRs, this should lie close to E_{QW} and indeed overlaps very satisfactorily with our E_{QW} data (i.e. our Bose-Einstein fit to E_{QW}, when extrapolated to higher temperatures, merges well with the linear fit to $E_{las(EEL)}$). Fig. 3 also gives the lasing energies, $E_{las(VCSEL)}$ (grey triangles), of actual operating VCSELs processed from the same wafer as sample A. One would normally assume this to be centered on the CM dip energy, E_{CM}, of the operating VCSEL (though, see later discussion). The dashed line is a linear fit to $E_{las(VCSEL)}$ with slope ~0.05meV/K, close to that obtained here for E_{CM} in sample A from the PR studies (0.043±0.002meV/K). However, our E_{CM} results for sample A are significantly higher than the $E_{las(VCSEL)}$ reported by [3] - by some 10meV. As a result, the resonance temperature indicated by the PR results (220±2K) is significantly lower than that suggested by the device results (~263K). Also, the PR studies show that the detuning between E_{QW} and E_{CM} at RT (~21meV) is also larger than that suggested by the device studies (~10meV) of [3].

To investigate the possible reasons behind this discrepancy, a piece from the edge of the sample A VCSEL wafer strip was cleaved off and annealed using the same technique and conditions as in [3]. A reflectance measurement was then performed at RT. Fig. 4 gives a comparison of the normalized R spectra before and after annealing. As can be seen, the annealing has caused a small red-shift in the CM dip position of ~3meV (12nm) from 0.534eV (2320nm) to 0.531eV (2332nm) but the main effect is to considerably broaden the CM dip. While the red-shift of 3meV is not sufficient in itself to account for the apparent 10meV difference between E_{CM} and $E_{las(VCSEL)}$ found in Fig. 3, the broader CM would have a pronounced effect on the spectral distribution of light leaving the device. In an ideal VCSEL, efficient lasing occurs at the lowest injection level for which the photon energy where the threshold gain condition is satisfied for which all losses are overcome. A

* Note these values were red-shifted by ~36meV by [3] in order to give the same alignment temperature of -10°C as reported by [2]

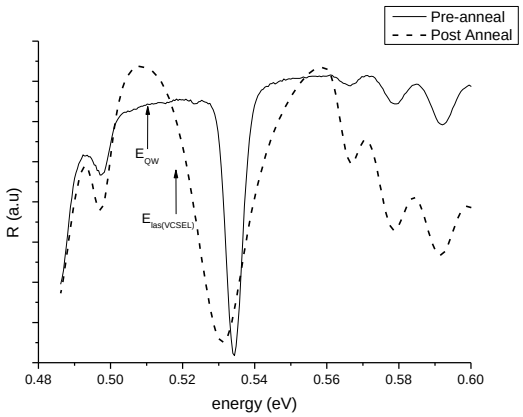

Fig. 4 Normal incidence 300K R spectra of pre-annealed (solid curve) and post-annealed (dashed curve) piece of sample A. CM dip is broadened after annealing and slightly red-shifted. Arrows show E_{QW} from PR, and $E_{las(VCSEL)}$ VCSEL lasing energy from [3].

broadened CM dip would allow a range of QW spectral emission to escape, the spectrum of which would result from a convolution of the QW gain spectrum and reflectivity CM profile, which may not necessarily peak at the lowest point of the CM dip. Referring to Fig. 4, at RT the PR measured E_{QW} energy is at ~0.51eV, lying to the left of the centre of the CM dip of the annealed sample, while the emission peak $E_{las(VCSEL)}$ lies somewhat closer to the CM dip at 0.52eV. We conclude, therefore, that the convolution of the QW gain spectrum peaking around E_{QW} and the broad VCSEL CM dip produces a lasing peak somewhat towards the lower energy side of the CM dip in the annealed VCSEL, at the position shown in Fig. 4 for $E_{las(VCSEL)}$ given by [3]. In these circumstances, the measurements of $E_{las(VCSEL)}$ by [3] might not be centered on E_{CM} due to the influence of this annealing, and it is too simplistic to assume that the observed VCSEL device lasing energy is exactly equal to the position of the CM dip minimum in the VCSEL structure. We note that other factors influence the lasing wavelength of the VCSEL devices, including band filling, particularly under high pumping conditions due to the presence of non-radiative[12], as may be expected in devices operating at longer wavelengths.

V SUMMARY AND CONCLUSIONS

We have made detailed spectroscopic characterizations of pre-fabrication 2.3μm GaSb-based VCSEL wafer sample, from 9K to 300K, clearly showing features associated with the CM dip and two QW transition energies, E_{QW} and E_{HOT}. Although the CM energy $E_{CM,}$ measured from angle dependent R at 300K, is at the desired emission wavelength of ~2.35μm (~0.52eV), E_{QW} is misaligned from E_{CM} by ~+21meV. However, cooling to 220±2K makes $E_{QW} = E_{CM}$ at ~0.532eV (~2.33μm). Our E_{QW} results agree well with separate measurements of the emission energy of EEL devices with similar active region [3], but the corresponding VCSEL device lasing energy is ~10meV lower than the E_{CM} found here. Reference [3] concludes the VCSEL, which was

fabricated from the same wafer as in the present study, has a resonance T of ~263K, higher than our predicted 220K. We demonstrated that the disagreement is likely caused by the VCSEL fabrication annealing process used in [3] which caused a broadening of the CM dip, red-shifting the VCSEL emission energy below the CM dip minimum. We concluded, therefore, that the convolution of this broadened CM dip and QW gain spectrum may contribute to a lowering of the emission energy, with other factors likely to play a role. Furthermore, this VCSEL emission energy does not truly reflect the position of the centre of the CM dip in the processed device, and lies somewhat below the actual $E_{CM.}$ Thus, one should be wary of interpreting the VCSEL device emission energy as a measure of E_{CM}.

The utility of the PR VCSEL characterisation technique is clearly demonstrated. To date, it is the only known non-destructive optical technique that can monitor the QW transition energies in full VCSEL structures. The study amply demonstrates the usefulness of PR for non-destructive pre-fabrication optical characterization in VCSEL manufacturing. Particularly, it demonstrates the degree of alignment between the QW gain peak and the cavity dip, and the temperature at which they can be brought into resonance, a condition of vital importance for the efficient and successful operation of VCSEL devices.

ACKNOWLEDGMENT

We acknowledge funding provided by the following: ‘Malaysian University Grant Program (GUP) Tier 1’, Universiti Teknologi Malaysia and M.O.H.E (grants Q.J130000.7126.01H55 and Q.J130000.7126.4D031); a UTM Zamalah Ph.D. scholarship for G. M. T. Chai; EPSRC(UK) and QinetiQ for funding for N.E. Fox; Petroleum Technology Development Fund (Nigeria) studentship for A. B. Ikyo; and Engineering and Physical Sciences Research Council (UK) grants EP/H005587/1 and GR/064725/01.

REFERENCES

[1] J. Bengtsson, J. Gustavsson, Å. Haglund, A. Larsson, A. Bachmann, K. Kashani-Shirazi, and M.-C. Amann, "Diffraction loss in long-wavelength buried tunnel junction VCSELs analyzed with a hybrid coupled-cavity transfer-matrix model," *Opt. Express*, vol. 16, pp. 20789-20802, 2008.

[2] A. Bachmann, K. Kashani-Shirazi, S. Arafin, and M. C. Amann, "GaSb-Based VCSEL With Buried Tunnel Junction for Emission Around 2.3μm," *IEEE Journal of Selected Topics in Quantum Electronics*, vol. 15, pp. 933-940, 2009.

[3] A. B. Ikyo, I. P. Marko, A. R. Adams, S. J. Sweeney, A. Bachmann, K. Kashani-Shirazi, and M. C. Amann, "Gain peak-cavity mode alignment optimisation in buried tunnel junction mid-infrared GaSb vertical cavity surface emitting lasers using hydrostatic pressure," *IET Optoelectron*, vol. 3, pp. 305-309, 2009.

[4] A. D. L. Cerutti, G. Narcy, P. Grech, G. Boissier, A. Garnache, E. Tourni é, F. Genty, "GaSb-based VCSELs emitting in the mid-infrared wavelength range (2–3μm) grown by MBE," *Journal of Crystal Growth*, vol. 311, pp. 1912-1916, 2009.

[5] P. Vicente, P. Thomas, D. Lancefield, T. Sale, T. J. C. Hosea, A. Adams, P. Klar, and A. Raymond, "Quantum Well and Cavity Mode Resonance Effects in a Vertical Cavity Surface Emitting Laser Structure, Observed by Photoreflectance Using Hydrostatic Pressure and Temperature Tuning," *physica status solidi (b)*, vol. 211, pp. 255-262, 1999.

[6] G. Blume, K. Hild, I. P. Marko, T. J. C. Hosea, S. Q. Yu, S. A. Chaparro, N. Samal, S. R. Johnson, Y. H. Zhang, and S. J. Sweeney, "Cavity mode gain alignment in GaAsSb-based near-infrared vertical cavity lasers studied by spectroscopy and device measurements," *Journal of Applied Physics*, vol. 112, pp. 033108-7, 2012.

[7] T. J. C. Hosea, "Advances in the application of modulation spectroscopy to vertical cavity structures," *Thin Solid Films*, vol. 450, pp. 3-13, 2004.

[8] O. J. Glembocki, "Modulation spectroscopy of semiconductor materials, interfaces, and microstructures: an overview," *Proceedings of SPIE*, vol. 1286, pp. 2-30, Aug 1 1990.

[9] S. A. Cripps, T. J. C. Hosea, S. J. Sweeney, D. Lock, T. Leinonen, J. Lyytikainen, and M. Dumitrescu, "High temperature operation of 760 nm vertical-cavity surface-emitting lasers investigated using photomodulated reflectance wafer measurements and temperature-dependent device studies," *IEE Proceedings - Optoelectronics*, vol. 152, pp. 103-109, 2005.

[10] S. A. Cripps and T. J. C. Hosea, "An enhanced model for the modulated reflectance spectra of vertical-cavity surface-emitting laser structures," *physica status solidi (a)*, vol. 204, pp. 331-342, 2007.

[11] K. P. O'Donnell and X. Chen, "Temperature dependence of semiconductor band gaps," *Applied Physics Letters*, vol. 58, pp. 2924-2926, 1991.

[12] K. Hild, I. P. Marko, S. R. Johnson, S. Q. Yu, Y. H. Zhang, and S. J. Sweeney, "Influence of de-tuning and non-radiative recombination on the temperature dependence of 1.3 mu m GaAsSb/GaAs vertical cavity surface emitting lasers," *Applied Physics Letters*, vol. 99, pp. 071110-3, 2011.